

## Supporting Information

### Simple, Green and High-yield Production of Single- or Few-layer Graphene by Hydrothermal Exfoliation of Graphite

Xiangrong Liu,<sup>b</sup> Mingtao Zheng,<sup>\*a</sup> Ke Xiao,<sup>b</sup> Yong Xiao,<sup>a</sup> Chenglong He,<sup>b</sup> Hanwu Dong,<sup>a</sup> Bingfu Lei,<sup>a</sup> and Yingliang Liu<sup>\*a</sup>

<sup>a</sup> College of Science, South China Agricultural University, Guangzhou 510642, China, E-mail: tliuyl@163.com, tliuyl@scau.edu.cn

<sup>b</sup> Department of Chemistry, Jinan University, Guangzhou 510632, P.R. China.

## 1. The quantitative yield of graphene under different hydrothermal conditions

As Fig. S1 shown, the graphene yield of 4 wt% under hydrothermal condition (513 K, 3.0 MPa) without  $\text{FeCl}_2$  is higher than the condition of 453 K (~ 2.1 wt%) and 573 K (~ 3.6 wt%), indicating that the temperature of close system is the key factor of exfoliation graphite. Comparing to exfoliate graphite under hydrothermal condition (513 K, 3.0 MPa) with  $\text{FeCl}_2$  and SDBS, the graphene yield is dramatically improved to ~10 wt%. Herein, we can conclude that  $\text{FeCl}_2$  can intercalate into graphene sheet to diminish van der waals interactions between graphite layers and facilitate exfoliation of graphene sheets. In addition, SDBS is employed to disperse graphene in the process of refrigeration of hydrothermal system.

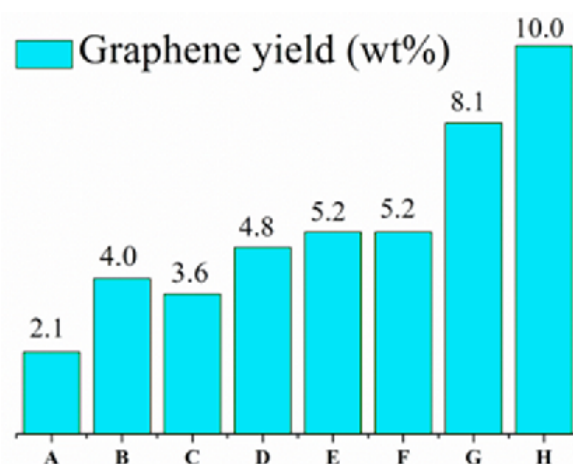


**Fig. S1** The quantitative yield of graphene under different hydrothermal conditions. A: exfoliation of graphite under hydrothermal condition (453 K, 0.8 MPa) B: exfoliation of graphite under hydrothermal condition (513 K, 3.0 MPa) with SDBS; C: exfoliation of graphite under hydrothermal condition (573 K, 8.0 MPa) with SDBS; D: exfoliation of graphite under hydrothermal condition (453 K, 0.8 MPa) with  $\text{FeCl}_2$ ; E: exfoliation of graphite under hydrothermal condition (513 K, 3.0 MPa) with  $\text{FeCl}_2$ ; F: exfoliation of graphite under hydrothermal condition (573 K, 8.0 MPa) with  $\text{FeCl}_2$ ; G: exfoliation of graphite under hydrothermal condition (573 K, 8.0 MPa) with  $\text{FeCl}_2$  and SDBS; H: exfoliation of graphite under hydrothermal condition (513 K, 3.0 MPa) with  $\text{FeCl}_2$  and SDBS.

## 2. X-ray diffraction (XRD) patterns of pristine graphite and graphene exfoliated by hydrothermal

In Fig. S2, the interlayer diffraction (002) peak of exfoliated graphite clearly downshifts compared to pristine graphite, and a dramatic decrease in the intensity of (002) peak of graphite can be observed. As the in-plane crystal structure of graphite retained, the broadening of (002) peak of the exfoliated graphite should be caused by decreased the thickness of graphite.

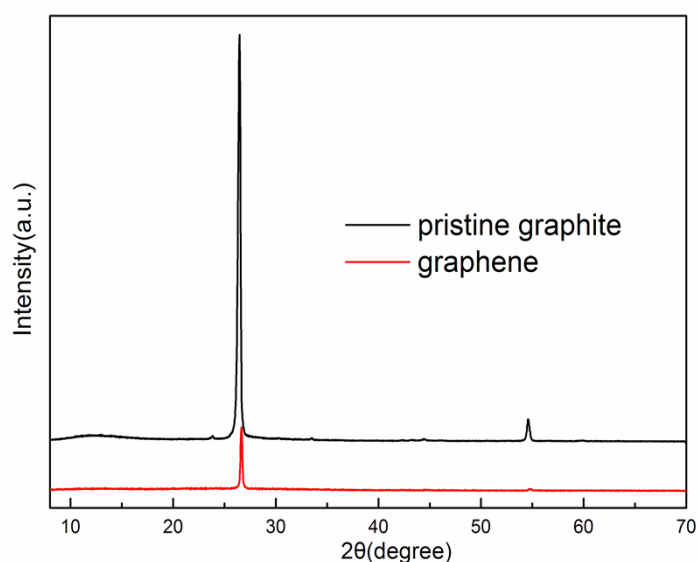
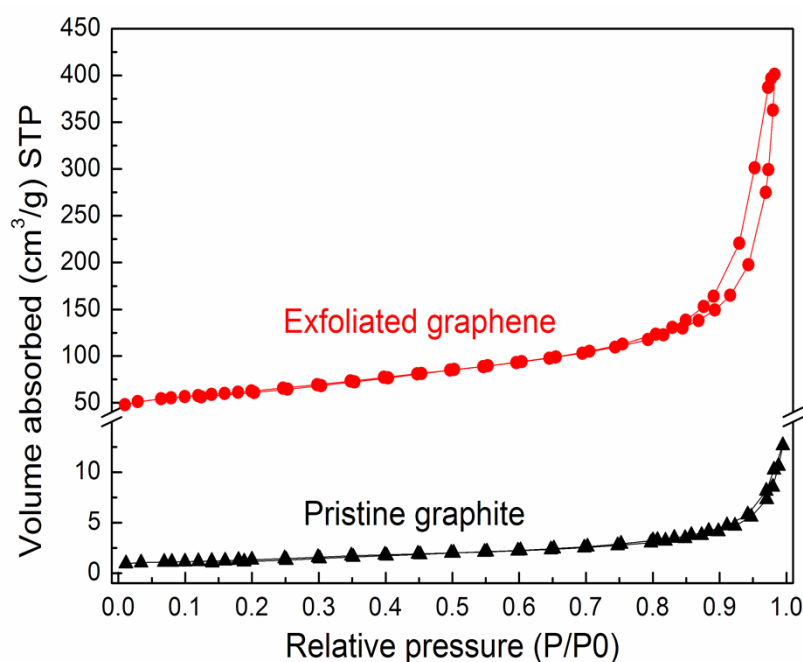


Fig. S2 X-ray diffraction (XRD) patterns of pristine graphite and graphene.

## 3. N<sub>2</sub> adsorption/desorption isotherms analysis of pristine graphite and graphene exfoliated by hydrothermal

The N<sub>2</sub> adsorption-desorption isotherms of pristine graphite and graphene were summarized in Fig. S3. All the samples were found to yield a type-II curve with steep uptakes up  $P/P_0 = 0.9$ , which indicated the materials has little pore. Before the relative pressure achieve to  $P/P_0 = 0.9$ , the amount of N<sub>2</sub> adsorption curve slowed

down, but when the relative pressure pass  $P/P_0 = 0.9$ , the curve increased sharply with increasing relative pressure, it was due to the materials of  $N_2$  adsorption capacity increased. The experimental results revealed that hydrothermal exfoliation of graphite leads to a dramatically increase in the BET surface area from  $3.6 \text{ m}^2 \text{ g}^{-1}$  for pristine graphite to  $217.3 \text{ m}^2 \text{ g}^{-1}$  for graphene.



**Fig. S3**  $N_2$  adsorption/desorption isotherms analysis of pristine graphite and graphene.

#### **4. The Raman spectra of exfoliated graphene collected at different sites**

The Raman spectrum (for more than 5 layers) becomes hardly distinguishable from that of bulk graphite<sup>1</sup>. Because the lateral resolution of the instrument was about  $1 \mu\text{m}$ , the Raman spectra results collected at different sites have not obviously differences and distinguishing. After carefully compared, the height of D peaks of the Raman spectra has distinction. Commonly, the D band of graphene indicates that the honeycomb crystal lattice and structure. The D peak ( $1,350 \text{ cm}^{-1}$ ) gives evidence of the

presence of defects, that is, either edges.

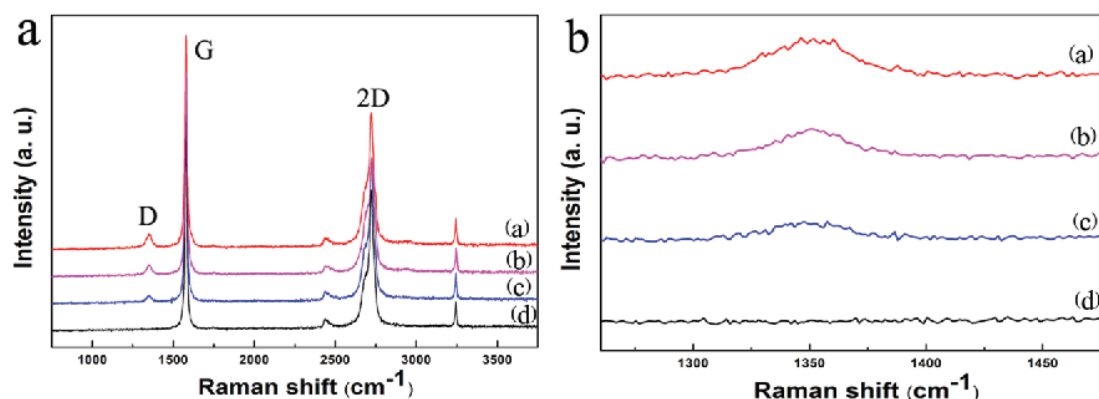
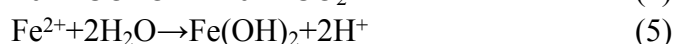
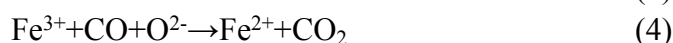
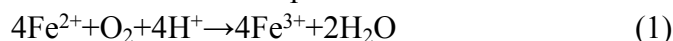


**Fig. S4** The Raman spectra of exfoliated graphene collected at different sites. The curve of (a) is the site of graphene edge, (b) and (c) are at the film of graphene, the curve of (d) is the Raman spectrum of graphene.

## 5. The evidence of the process of divalent ion ( $\text{Fe}^{2+}$ ) in hydrothermal water

It can be considered that Fe species still maintain divalent ion in hydrothermal water. Pure  $\text{N}_2$  was used to replace the air in the reactor. There have many reductive raw materials such as C and Fe (from the reactor made by 316SS stainless steel). Those can maintain  $\text{Fe}^{2+}$  in hydrothermal water, although a bit of  $\text{Fe}^{2+}$  would be oxidized to  $\text{Fe}^{3+}$ . The possible reactions of  $\text{Fe}^{2+}$  during the process were as follows:



There is some dissolved oxygen in the reaction system, and the dissolved oxygen can be reacted with  $\text{Fe}^{2+}$  to  $\text{Fe}^{3+}$  (Eq. 1), and with C to generate CO (Eq. 2) during the hydrothermal process. Owing to the reducibility of C, CO, and Fe in the system, the generated  $\text{Fe}^{3+}$  will be reduced to  $\text{Fe}^{2+}$  (Eqs. 3 and 4). On the other hand, it is well-known that  $\text{Fe}^{2+}$  can be hydrolyzed to  $\text{Fe}(\text{OH})_2$  in water system, but the generated acid ( $\text{H}^+$ ) can inhibit this hydrolysis process (Eq. 5). Therefore, it is safe to be considerable that  $\text{Fe}^{2+}$  can maintain divalent ion in hydrothermal water coexisting of C and Fe.

To further support the above conclusion, the sediments obtained from different starting materials were investigated by FTIR analyses. Fig. S5a shows the FTIR spectrum of crystalline  $\text{FeCl}_2$ , from which four typical absorption peaks around 1615, 1406, 1057, and 585  $\text{cm}^{-1}$  can be observed. These peaks can also be observed in the spectra of the products obtained from hydrothermal treatment of  $\text{G} + \text{FeCl}_2$  (Fig. S5d) and  $\text{G} + \text{SDBS} + \text{FeCl}_2$  (Fig. S5e), also indicating the presence of  $\text{FeCl}_2$  in the final sediments after hydrothermal treatment. It is noted that a new peak around 863  $\text{cm}^{-1}$  can be seen in the sample obtained from starting materials with additive of  $\text{FeCl}_2$ , including  $\text{G} + \text{FeCl}_2$  and  $\text{G} + \text{SDBS} + \text{FeCl}_2$ , as shown in Fig. S5 e and f (denoted by ■). This peak comes from the bending vibration of C-H in aromatic ring, indicating that

the presence of  $\text{FeCl}_2$  can facilitate the exfoliation of graphite.

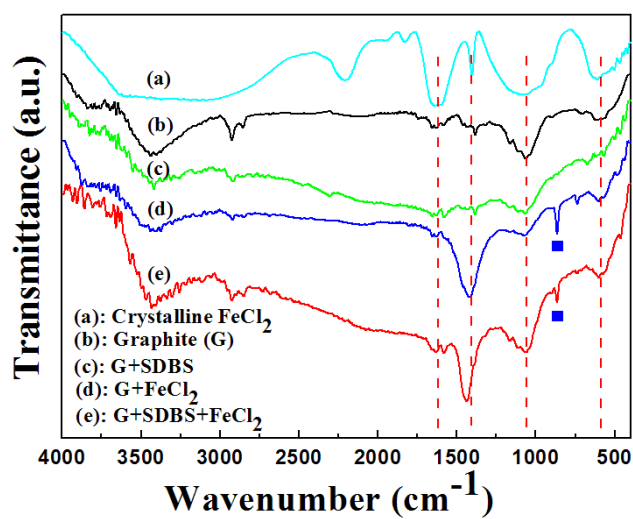


**Fig. S5** FTIR spectra of the samples of (a) crystalline  $\text{FeCl}_2$ , (b) graphite (G), (c) G+SDBS, (d) G+ $\text{FeCl}_2$ , and (e) G+SDBS+ $\text{FeCl}_2$ .

## 6. References

[1] M. Lotya, Y. Hernandez, P. J. King, R. J. Smith, V. Nicolosi, L. S. Karlsson, F.M. Blighe, S. De, Z.M. Wang, I.T. McGovern, G.S. Duesberg, J.N. Coleman, Liquid phase production of graphene by exfoliation of graphite in surfactant/water solutions. *J. Am. Chem. Soc.* **2009**, 131, 3611-3620.